



Phase Transformations in Silicon Under Dry and Lubricated Sliding[©]

ANDRIY KOVALCHENKO (Member, STLE)

University of Illinois at Chicago
Department of Mechanical Engineering
Chicago, Illinois 60607

and

YURY GOGOTSI and VLADISLAV DOMNICH

Drexel University
Department of Materials Engineering
Philadelphia, Pennsylvania 19104

and

ALI ERDEMIR (Member, STLE)

Argonne National Laboratory
Energy Technology Division, Tribology Section
Argonne, Illinois 60439

Sliding friction and wear mechanisms of silicon/silicon nitride test pairs were investigated under conditions of both dry and lubricated sliding. High-resolution surface topography mapping and electron microscopy studies revealed that microfracture was the predominant wear mechanism under dry and grease-lubricated sliding conditions. Raman spectroscopy suggested that in certain areas of the sliding contact, silicon underwent phase transformation and reached a metallic state because of high contact pressures. The extent of phase transformation was greater during the very early stages of the run-in period than during steady-state sliding regimes.

The use of grease and oil as lubricants led to a substantial reduction in friction and greatly diminished wear due to microfracture. Furthermore, almost all areas on Si surfaces subjected to lubricated sliding contact underwent pressure-induced phase transformation. Both amorphous material and crystalline Si phases were identified by Raman spectroscopy. The experimental observations suggested that the wear process in lubricated sliding contacts was mainly dominated by the formation of a ductile metallic Si phase and subsequent removal of the transformed layers.

The results of this study demonstrate that pressure-induced phase transformation must be taken into account when considering possible wear mechanisms of silicon in contact with other hard materials, inasmuch as it contributes notably to the wear of silicon under lubricated sliding.

KEY WORDS

Silicon; Ceramics; Boundary Lubrication; Phase Transformations; Raman Spectroscopy; Wear Mechanism

INTRODUCTION

Silicon is the primary material for fabrication of integrated circuits, microelectromechanical systems (MEMS), and many optical and optoelectronic devices, which emphasizes the importance of the investigation of sliding contact behavior of silicon against other materials. In particular, the tribological properties of silicon have received extensive attention in recent years mainly because of their major role in machining, chemo-mechanical polishing, and MEMS applications. Mishina (Mishina, 1988) studied the friction and wear behavior of silicon in contact with several pure metals from the tribochemical viewpoint and determined that chemical affinity and the Schottky barrier height between the metal and semiconducting silicon were key factors in their contact interactions. Park, et al. (Park, 1991) studied the transition from brittle to ductile deformation mode in sliding of single-crystal silicon wafers against a partially stabilized zirconia ball at various temperatures, and established, by means of scanning electron microscopy (SEM), the formation of cracks at 25° and 300°C, and dislocation arrays at 600°C in the subsurface layer of the affected

Presented at the 56th Annual Meeting
in Orlando, Florida
May 20-24, 2001

Final manuscript approved March 13, 2002
Review led by Robert Fusaro

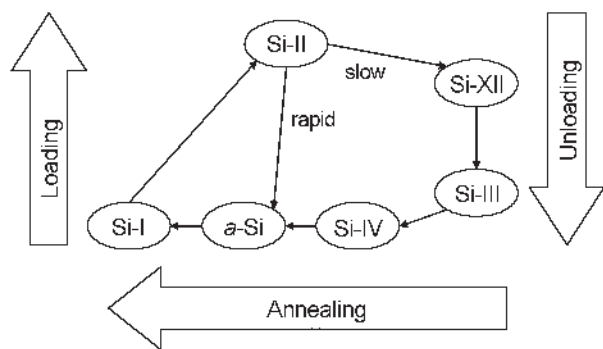


Fig. 1—Schematic representation of phase transformations occurring in silicon under contact loading and during subsequent heat treatment.

material. It was inferred that the change in deformation mode from brittle fracture to plastic flow accounted for the differences in wear and was probably related to thermal activation of dislocations as the temperature was increased (Park, 1991).

Zanoria, et al. (Zanoria, 1993; Zanoria, 1995a; Zanoria, 1995b) observed the formation of cylindrically shaped wear debris (“rolls”) during sliding of a polycrystalline silicon ball against a silicon flat. Transmission electron microscopy (TEM) analysis revealed that the rolls were made of amorphous silica. The authors concluded that these rolls resulted from oxidation of silicon during preparation of the flat and the ball samples and during experiments in humid environments. The presence of SiO_2 rolls at the sliding interface effectively reduced the friction and wear rates and helped to maintain them at low steady-state values.

Most of the tribological studies on silicon have explored its abrasive scratching behavior in contact with sharp or blunt indenters. To quantify the mechanical damage produced in linear scratches by Vickers and spherical diamond tips that simulated the single point contact of the cutting tools, Danyluk, et al (Danyluk, 1988; Kim, 1990; Li, 1996) developed a technique to measure electrical resistivity. The relative changes in voltage were correlated with the time for the diamond to move past the probes; and the time was shown to depend on the dead load on the diamond tip and on the properties of silicon (Li, 1996). SEM analysis of scratches showed that the scratch morphology depended on temperature (Danyluk, 1988): as the temperature was increased, the grooves became shallower and displayed evidence of plowing.

SEM analysis of silicon wafers after single-point diamond turning (Blackley, 1994; Blake, 1990) and linear scratching with diamond tools (Bhushan, 1997; Scott, 1992) revealed signs of plastic deformation, even at room temperature. Such ductile behavior was unexpected because silicon generally exhibits limited dislocation mobility and brittle behavior below 650°C . TEM studies of scratches produced in silicon wafers with sharp diamond indenters (Minowa, 1992; Morris, 1994) revealed a thin layer of amorphous material along the grooves, with a lightly dislocated/median-cracked region just beneath the amorphous layer. The amorphized zone was apparently equal to the contact area,

and under given experimental conditions (maximum loads of 10–20 mN), it extended to depths of 150–200 nm beneath the specimen surface.

The presence of amorphous material in the surfaces subjected to contact loading has been shown to correlate with the pressure-induced metallization of silicon under the diamond indenter (Domnich, 2001a). It is known that at hydrostatic pressures of ≈ 12 GPa, silicon transforms from the semiconducting phase with cubic diamond structure (Si-I or *cd*) into a ductile metallic phase with the β -tin structure (Si-II) (George, 1999). Extensive experimental data obtained from hardness impressions on silicon suggest that a similar transformation occurs during the indentation tests (Bradby, 2001; Callahan, 1992; Clarke, 1988; Gogotsi, 2000; Gridneva, 1972; Gupta, 1980; Kailer, 1997; Pharr, 1992; Weppelmann, 1993). Furthermore, metallic Si-II is metastable under ambient conditions and transforms upon unloading into amorphous material (*a*-Si) or crystalline polymorphs of silicon (Si-III or *bc8*, body-centered cubic structure with eight atoms per unit cell; Si-XII or *r8*, rhombohedral structure with eight atoms per unit cell; and Si-IV or *hd*, hexagonal diamond structure) depending on the pressure-release conditions (Domnich, 2001a). The entire transformation path of silicon during indentation is illustrated in Fig. 1. Moreover, recent results by Gogotsi et al. suggest that the room-temperature ductile behavior of silicon observed during scratching (Gogotsi, 2001) and under various machining operations (Domnich, 2001b; Gogotsi, 1999) is also controlled by pressure-induced metallization under the moving tool.

All previous observations of contact loading-induced phase transformations in silicon involved a contact between the specimen surface and a relatively sharp diamond indenter or a tool that contained sharp diamond grains. Small contact areas in these cases led to highly localized contact stresses that enabled the Si-I \rightarrow Si-II transformation under the tool. However, no information was available on whether the metallization of silicon can be attained by using softer counterface materials and under less localized loading. In this study, the authors attempt to determine the mechanism of silicon wear in contact with a large-radius silicon nitride ball, paying special attention to possible signs of silicon metallization during the standard tribological experiments. Taking into account the successful use of Raman microscopy for the determination of phase compositions and residual stresses in silicon surfaces subjected to contact loading (Bradby, 2001; Domnich, 2000; Gogotsi, 2000; Gogotsi, 1997; Kailer, 1997; Tanikella, 1996), the authors selected this technique as the primary characterization tool for the present research.

EXPERIMENTAL PROCEDURE AND MATERIALS

In the authors experiments, they use 0.7 mm-thick single-crystal (111) *p*-type silicon wafers supplied by Mitsubishi Silicon America. The wafer surfaces were polished and etched according to semiconductor industry standards, and had a specified surface roughness of $R_a = 0.005 \mu\text{m}$, RMS. Standard ball-bearing-grade silicon nitride (Si_3N_4) balls were used as the pin material. The diameter of the balls was 9.55 mm (0.375 in.).

The friction and wear tests were carried out in a ball-on-disk tribometer under dry and lubricated sliding conditions at room

TABLE 1—PROPERTIES OF MULTI-PURPOSE LITHIUM GREASE		
PROPERTY		SPECIFIC VALUE
Viscosity at	40°C	124 cSt
	100°C	12.8 cSt
Penetration at	60 strokes	280
	10,000 strokes	287
Dropping point, °C		191
PROPERTIES OF POLYALPHAOLEFIN SYNTHETIC OIL		
PROPERTY		SPECIFIC VALUE
Viscosity at	40°C	18 cSt
	100°C	4 cSt
Pour Point		-57°C
Flash Point		218°C

TABLE 2—WIDTH OF WEAR TRACKS ON SILICON AFTER SLIDING IN CONTACT WITH SILICON NITRIDE AT VARIOUS LOADS (LINEAR VELOCITY, 30 mm/s; EXPERIMENT DURATION, 10 min)		
LOAD, N	WIDTH OF WEAR TRACKS, μm	
	DRY SLIDING	BOUNDARY SLIDING
1	230 \pm 5	190 \pm 4
2	290 \pm 7	200 \pm 5
5	340 \pm 8	335 \pm 8
10	-	360 \pm 9
20	-	420 \pm 10

temperature (22 °C). The test specimens were mounted inside a plexiglas chamber to provide a controlled test environment. Dry sliding experiments were conducted in open air (with 40% relative humidity) and dry nitrogen (derived from a liquid nitrogen tank), while lubricated tests were performed in open air using a base synthetic oil and a commercial grease. The type of oil and grease as well as their properties are provided in Table 1. The dead weights used during sliding experiments varied between 1 and 10 N in order to achieve a wide range of contact pressures. The linear velocity ranged from 5 to 30 mm/s. The reason for using such low linear velocities was primarily to diminish the extent of frictional heating and thus to suppress possible tribochemical reactions as well as establish and maintain a boundary lubrication regime under oil or grease lubricated sliding conditions. In these tests, Si_3N_4 balls were rubbed against the single-crystal silicon wafers. The wear track diameter was 10 mm. Under these experimental conditions, wear damage was restricted to mechanical fracture and pressure-induced phase transformations. The friction force was monitored continuously with a data acquisition system, which allowed calculation of friction coefficients throughout the test. Each test was repeated at least three times to verify the repeatability of the friction and wear data.

After the tribological tests the worn surfaces were investigated and the wear tracks on the silicon disks and the wear scars on the Si_3N_4 balls were analyzed by optical microscopy, SEM, and quantified by optical profilometry. Phase compositions of the worn surfaces of the silicon were determined by Raman spectroscopy. For this purpose, a Raman microspectrometer equipped with an argon-ion laser (514.5-nm excitation wavelength) and a charge-coupled device detector were used. The silicon wafers and silicon nitride

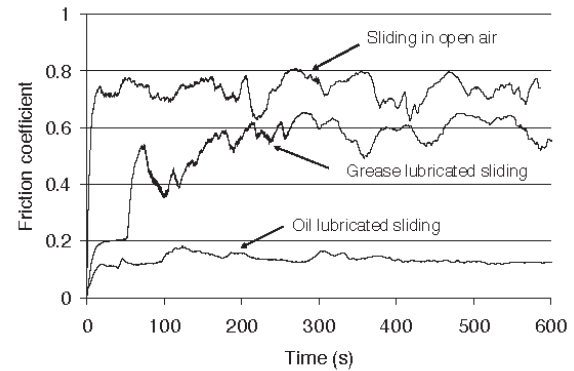


Fig. 2—Typical behavior of friction coefficient of silicon-silicon nitride couple under dry friction, grease, and oil-lubricated conditions.

balls were thoroughly cleaned in acetone and methanol in an ultrasonic bath before tribological tests.

EXPERIMENTAL RESULTS

Friction and Wear Behavior in Air

Initial tribological experiments were performed under dry sliding conditions at a 30-mm/s linear sliding speed and at contact loads of 1, 2, and 5 N. The duration of each friction test was 10 min. Use of higher loads was difficult because of the premature failure of silicon wafers after the sliding motion began. The authors believe that high contact pressures coupled with high friction coefficients (i.e., 0.6-0.8) were major reasons for the premature fracture of silicon. At all contact loads, the friction coefficients rapidly increased after a brief run-in period and then fluctuated between 0.6 and 0.8. A typical open-air friction coefficient-*vs.*-time dependence is shown in Fig. 2.

Microscopic examination of the worn surfaces confirmed widespread microfracture on the sliding contact areas of the silicon wafers and Si_3N_4 balls. The depth and width of the wear tracks on silicon wafers increased with increasing contact load (Table 2). The width of the wear scars on the Si_3N_4 balls also increased with load and roughly corresponded to the width of the wear tracks on the silicon wafers. Raman microanalysis of the worn silicon surfaces after the friction tests in open air generally did not reveal signs of structural changes within the affected material. Fig. 3 shows the Raman spectra of wear tracks formed on silicon wafers during sliding against Si_3N_4 balls in open air. Figures 3(a) and 3(b) show the Raman features of those areas that exhibited mostly brittle fracture, while Fig. 3(c) was taken from a plastically deformed area in the wear track. Areas indicative of brittle fracture and plastic flow are identified with arrows in optical and SEM images in Figs. 4 and 5.

Each spectrum in Figs. 3(a)-3(c) shows a Raman band at $\approx 520 \text{ cm}^{-1}$, which corresponds to the triple degenerate zone-center (Γ point) phonons of Si-I phase in Fig. 1. Certain areas along the wear tracks displayed more pronounced two-phonon scattering in Si-I (L and X points), as well as a split Si-I (Γ) peak that was the result of a complex stress state in a particular point associated with cracking (Fig. 3(a)). Such a microfracture-dominated wear mech-

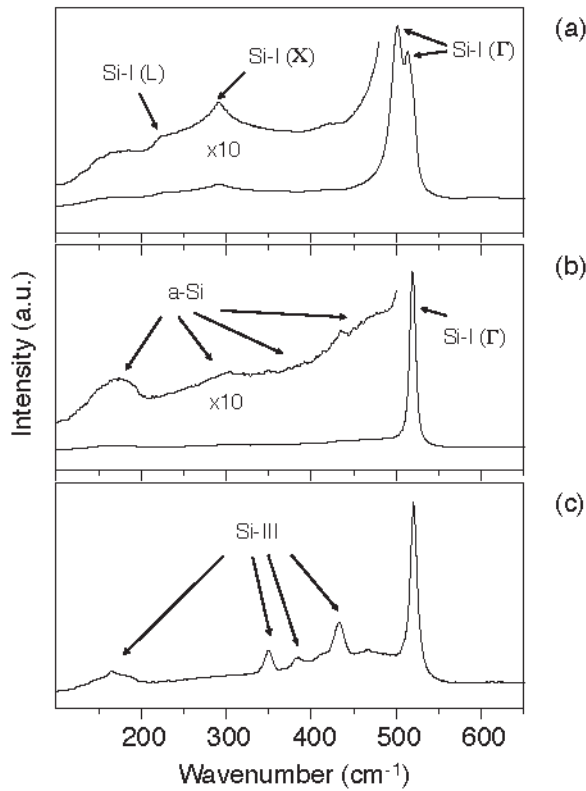


Fig. 3—Raman spectra recorded from silicon wear tracks after dry friction against a Si_3N_4 ball.
 (a) area of mostly brittle fracture
 (b) area of mostly brittle fracture
 (c) plastically deformed area (Area A in Fig. 5)

anism is consistent with the very brittle nature of silicon in the absence of lubrication. The authors note here that although the Raman spectra of the wear tracks produced during sliding contact in open air were dominated by the bands of Si-I, the traces of amorphous silicon (Maley, 1988) (broad bands at 160, 310, 400 and 470 cm^{-1} , Fig. 3(b)) and/or the crystalline Si-III phase (Hanfland, 1990; Olijnyk, 1999) (bands at 166, 350, 384, and 435 cm^{-1} , Fig. 3(c)) were also observed in certain points along the wear tracks.

To investigate how the scale effect alters the mechanism of the wear of silicon, additional tribological experiments were performed at lower contact loads and lower linear velocities (1 N and 5 mm/s, respectively, the minimum possible load and speed values available for the test apparatus used in this study). Duration of the experiments was 1, 10, and 20 min. The sliding frictional behavior of these test pairs was the same as that observed in the earlier experiments at higher loads and velocities. Specifically, after a rapid increase during the first few seconds, the friction coefficients began to fluctuate between 0.4 and 0.6. As expected, the wear of Si_3N_4 balls and silicon disks increased with increasing sliding time (see Figs. 4(a), 4(b), and 4(c)), a finding that is related to the augmentation of brittle fracture with increasing test duration. Meanwhile, SEM images of selected areas within the wear

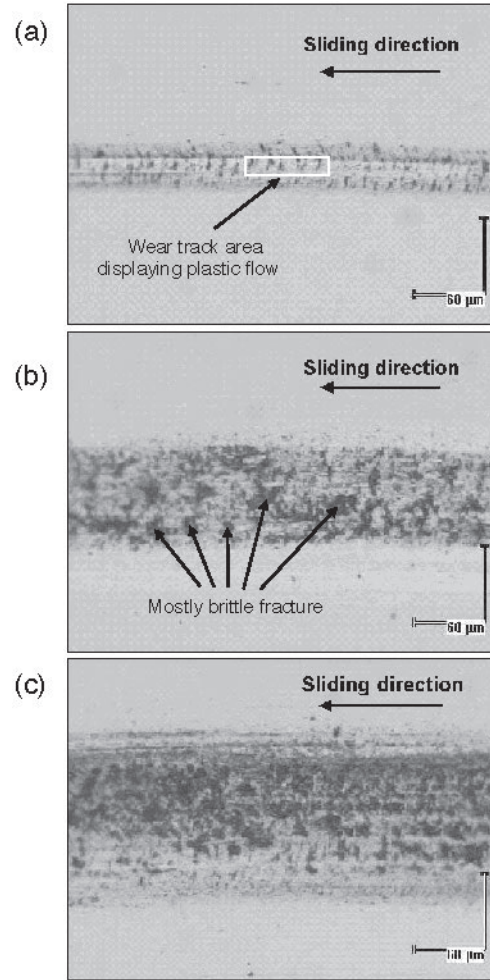


Fig. 4—Optical images of worn silicon surfaces after friction in air.
 (a) 1 min
 (b) 10 min
 (c) 20 min under 1-N load and 5-mm/s linear sliding velocity

tracks on a silicon disk subjected to a 1-min friction test clearly revealed evidence of some plastic and/or viscous flow in the center of the wear track (Fig. 5(a)). Specifically, area A in Fig. 5(a) is characterized by a very smooth sliding surface, relatively lower amount of small cracks compared to the surface that was closer to the edge of the wear track, and it has a typical appearance of a plastically deformed worn surface of a metal. The Raman spectra taken from the corresponding areas show pronounced features associated with the crystalline Si-III phase and amorphous silicon (Fig. 3(c)). Inasmuch as the Si-III phase can be formed only via the metallic Si-II phase, this observation confirms partial pressure-induced metallization of silicon during sliding tests in open air, leading to the plastic flow of the ductile metallic phase as evident from Figs. 5(a) and 5(b).

After 10 and 20 min of sliding, a predominantly brittle character of wear was revealed by optical microscopy, SEM, and Raman spectroscopy studies. From this observation, the authors conclude that a transformed layer formed at early stages of the friction test is later removed because of wear by brittle failure.

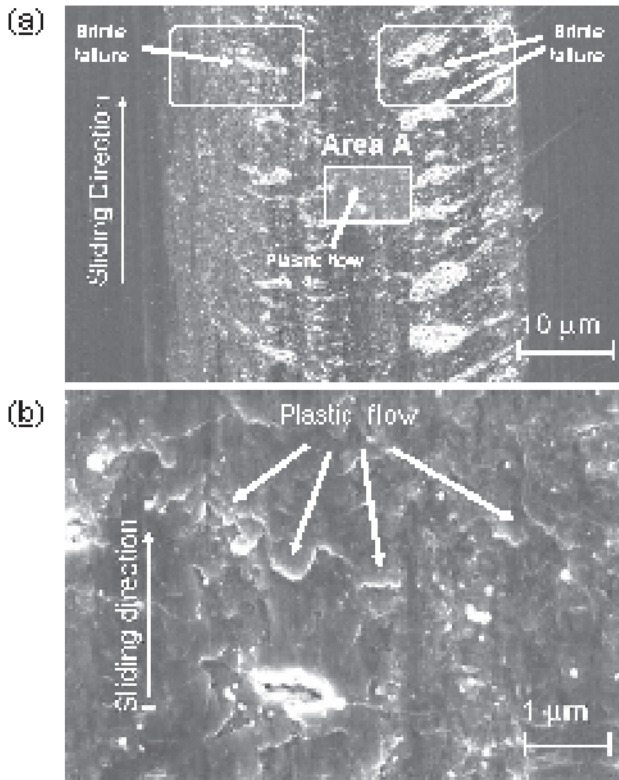


Fig. 5—SEM images of worn silicon surfaces after friction in air during 1 min under 1-N load and 0.005-m/s linear sliding speed.

- (a) general view
(b) area of plastic flow (Area A)

Friction and Wear Behavior in Dry Nitrogen

The purpose of these experiments was to eliminate the possible effects of water and oxygen molecules on friction and wear of silicon wafers during sliding against Si_3N_4 . As mentioned in the introduction, the presence of oxygen and water molecules in the test environment may lead to the formation of SiO_2 on sliding surfaces of both the silicon and Si_3N_4 , and the oxidized wear debris particles trapped at the sliding interface may play a significant role in the friction and wear behavior of these materials. Except for the test environment, the other test conditions were kept the same as in the test run in humid air (i.e., 1, 10, and 20 min sliding time, 1-N contact load, and 5-mm/s linear speed). Raman spectroscopy and microscopy of worn surfaces revealed that the morphology and composition of the worn surfaces did not differ significantly from those obtained in air. The friction and wear behavior of test pairs tested in dry nitrogen was also similar to that observed in air. These results imply that the surface oxidation under the experimental conditions of the present study either did not occur or did not significantly affect the sliding friction and wear behavior.

Friction and Wear Behavior Under Lubricated Test Conditions

In an attempt to reduce the effects of microfracture on friction and wear, and to expand the range of sliding contact regimes from

dry sliding (in air and dry nitrogen) to boundary lubrication, the authors used a commercial grease and a base synthetic oil to lubricate the sliding contact surfaces of the test pairs.

Test with Grease Lubricated Surfaces

Tests with grease lubricated surfaces were performed with a multi-purpose white lithium-base grease. The general properties of this grease can be found in Table 1. The applied load in the grease-lubricated experiments was 1 N. The linear velocity was 30 mm/s and the test duration was 10 min.

The use of grease as a lubricant in sliding contact experiments did not necessarily reduce the friction and the predominantly brittle character of the wear process. The authors noted that the increase in friction coefficient was rather slow in the beginning of the test (Fig. 2). The average width of the wear track on a silicon wafer after sliding with grease was equal to 225 μm . The deviation in the widths of the wear tracks upon subsequent experiments did not exceed 5%. SEM images of the wear tracks on silicon are similar after the experiments with and without lubrication, but the areas displaying amorphous silicon on the worn surface (as revealed by Raman spectroscopy) are more often observed in this case than in the unlubricated sliding tests. Thus, although some plastic flow via pressure-induced metallization occurred in silicon during sliding with grease, brittle fracture remained as the predominant wear mechanism in this case, mainly because insufficient lubricating ability of the chosen grease (especially after run-in period) has led to a high frictional force which caused microcracking. Looking at the wear tracks, the authors could easily see the total removal of grease from the sliding contact areas of the silicon wafer and the formation of a deep wear groove. Si_3N_4 ball also wore during grease lubricated sliding tests and a wear scar was present on its contact spot. These wear scars had a circle shape and their width roughly corresponded to the width of the wear track on silicon wafer.

Tests with Oil Lubricated Surfaces

This series of experiments was aimed at studying the wear mechanism of silicon when the friction force can be significantly reduced by the presence of oil. In the authors experiments, silicon wafers were placed in a special bath filled with a base synthetic oil, poly α -olefin (PAO) without any additives. The general properties of this oil can be found in Table 1. Each experiment lasted for 10 min and was performed under linear velocity of 30 mm/s and loads of 1 - 20 N. Considering the point contact between Si_3N_4 ball and silicon wafer combined with high contact loads and fairly slow sliding speeds, one should expect a boundary lubricated regime in these experiments. In particular, the range of friction coefficients, i.e., 0.1-0.2 (Fig. 2), was typical of boundary lubricated sliding regimes. Conversely, if the sliding was taking place under hydrodynamic and/or elastohydrodynamics regimes, then a direct contact between the Si_3N_4 ball and silicon wafer would not exist and the formation of deep wear grooves on silicon wafers and wear scars on Si_3N_4 balls would not be observed.

Unlike grease lubrication, lubrication of sliding surfaces with a base PAO oil permitted experiments to be run under significantly higher loads without triggering brittle fracture of the sliding silicon surfaces. Friction coefficients in all tests were mostly steady

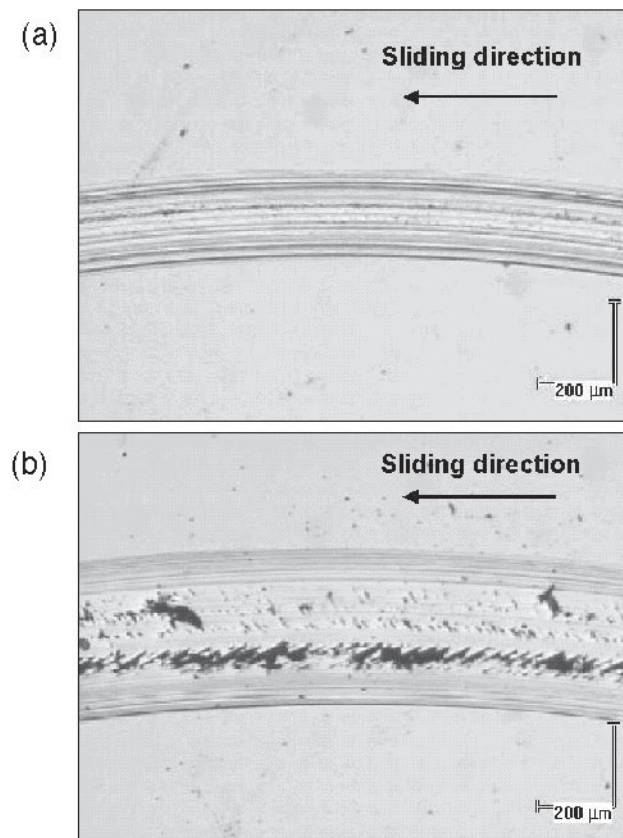


Fig. 6—Optical images of silicon wear tracks after friction in contact with Si_3N_4 ball under boundary lubrication.
(a) 2 N
(b) 10 N loads

and did not exceed 0.2 (Fig. 2). Noise was essentially absent and the frictional traces were rather smooth in all cases. It should be noted that microfracture was absent on the silicon wear tracks after tests at 1 and 2 N. Cracks developed only at or above a 5 N load. Figure 6 shows that with increasing normal load, the wear tracks on silicon surface become wider and more cracks form on the sliding surfaces. The widths of the wear tracks on silicon wafers are given in Table 2.

The wear scars on the Si_3N_4 balls were different from those reported for the unlubricated and grease-lubricated cases: the volumetric wear of the Si_3N_4 ball side was negligible and the ball maintained its spherical shape in the case of oil-lubricated tests. Under microscope, it looked as if the ball had established a line contact over the grooved wear track on the silicon disk after the running-in stage. On the ball side, the authors could only find some longitudinal scratches with an alignment parallel to the sliding direction. In short, only silicon was worn out during the sliding contacts in oil lubricated tests. The cross-section profile of the wear tracks on silicon wafers recorded with the aid of the optical profilometer shows a nearly circular shape that mimics the spherical shape of the Si_3N_4 balls (Fig. 7). The heights and widths of the microscopic longitudinal parallel grooves on the wear track (Fig. 7(b)) are the same as those grooves that were found on Si_3N_4 balls. This observation is in contrast to the results of unlubricated tests

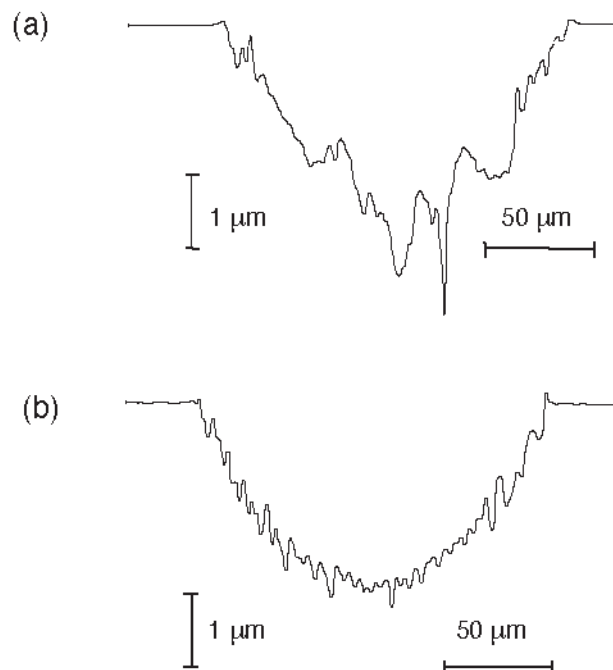


Fig. 7—Relief of wear tracks on silicon plates after friction against Si_3N_4 ball under (a) and (b).
(a) dry friction
(b) boundary lubrication at 5 N load

with Si_3N_4 balls where a truncated sector of the material was removed from the ball surfaces by wear and a cross-section profile of the silicon wear track is very far from circular (Fig. 7(a)).

Figure 8 shows typical SEM images of the wear tracks on Si produced under boundary lubrication and at a sliding velocity of 30 mm/s. SEM analysis reveals that the worn surface of silicon, especially at low loads, is completely covered by a smooth layer, with only negligible amounts of cracking. Also, clearly seen in Fig. 8(a) is the evidence of plastic flow of silicon under the spherical ball. Raman spectroscopy (Fig. 9) indicates that this plastically deformed layer on top of the wear track consists mostly of amorphous material. The band of Si-I at 520 cm^{-1} (Fig. 9) is effectively suppressed when compared with the bands of α -Si ($160, 300, 390, \text{ and } 470\text{ cm}^{-1}$), and in many cases is hardly distinguishable in the Raman spectra of the wear tracks (Fig. 9(c)). After reaching some load threshold (5 N under these experimental conditions), the cavities on the silicon surface start to appear in addition to the plastically deformed layer. From the SEM image in Fig. 8(b), noticing the regularity and parallel orientation of the cracks, the authors can affirm that these cracks were initiated along the crystallographic planes. Also, it is evident that the cause for cracking is the increased normal force, which accordingly increases contact pressure, in contrast to friction without lubrication, where the main cause for cracking was a high tangential force.

DISCUSSION

Room-temperature fracture toughness of silicon is on the order of $0.9\text{ MPa m}^{1/2}$ (Roberts, 1999), therefore, it is not surprising that

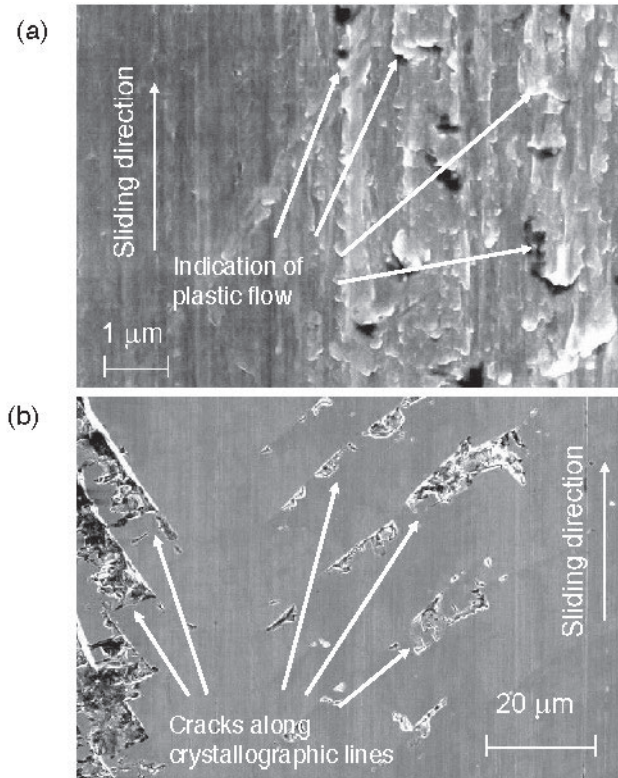


Fig. 8—SEM images of amorphous layer on worn surface of silicon. (a) after friction in contact with Si_3N_4 under conditions of boundary lubrication at 1-N load (b) cracking in (001) silicon in the central part of the wear track at 10-N load

the wear of silicon is largely dominated by microfracture. With increasing temperature, silicon undergoes a brittle-to-ductile transition at temperatures $>500^\circ\text{C}$ (Roberts, 1999). This transition is associated with increasing plastic flow due to dislocation nucleation and motion. During tests in open air and at elevated temperatures, surface oxidation may also take place in silicon. Scuffing or microseizure is not expected to occur on the sliding silicon surfaces, at least to a noticeable extent. Thus, some other mechanism should be responsible for the observed plasticity of silicon during sliding and machining at ambient temperature.

The authors maintain here that under certain experimental conditions, the high stresses associated with the sliding contact between a silicon flat and a Si_3N_4 ball are sufficient to initiate the Si-I \rightarrow Si-II transformation (see Fig. 1) within the affected area. It is the ductile metallic Si-II phase that deforms plastically under the Si_3N_4 ball and leads to the characteristic morphologies shown in Figs. 5 and 8(a). The surface morphology is preserved after the load is withdrawn; however, the outermost layer of the wear tracks consist of amorphous silicon or a crystalline Si-III phase which both form from metallic Si-II depending on the unloading conditions behind the moving Si_3N_4 ball.

Overall, the results of this study demonstrate that the pressure-induced metallization of silicon is feasible during sliding against Si_3N_4 , provided that the experimental conditions are favorable.

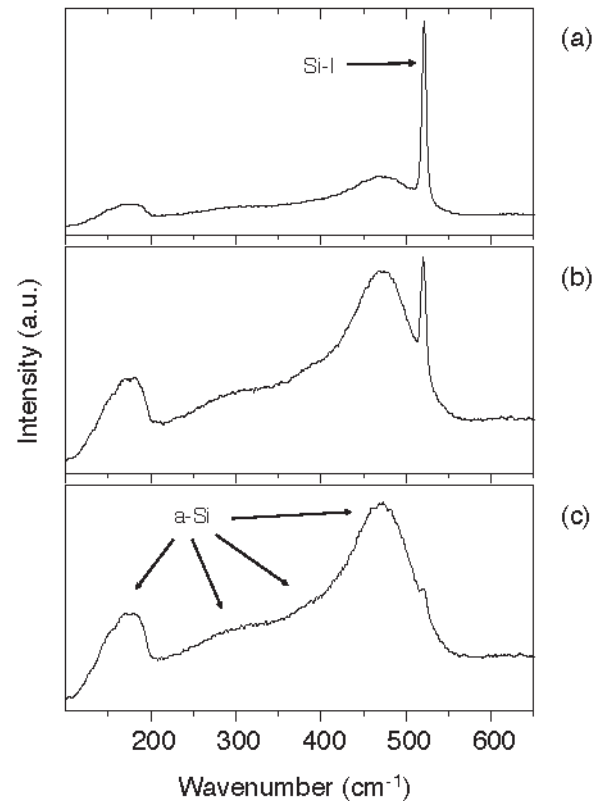


Fig. 9—Typical Raman spectra recorded from the uncracked areas on the wear track on silicon after sliding contact with a Si_3N_4 ball under boundary lubrication conditions.

The results also show that microfracture is by far the largest contributor to the wear of silicon (especially under dry sliding conditions). SEM investigation of wear tracks revealed two types of cracks on wear tracks. One type was aligned at an angle to the sliding direction (see Figs. 5(a) and 9(b)) and was mostly associated with weak cleavage planes of the silicon wafer. The second type was perpendicular to the sliding direction (see Figs. 4 and 5) and was most likely due to high frictional traction and hence tensile forces developing behind the moving asperities of Si_3N_4 balls. As reported by Hamilton and Goodman (Hamilton, 1966), under sliding conditions where friction coefficient exceeds 0.3, the maximum shear stress is shifted from the subsurface toward the sliding surface. The higher the friction coefficients, the greater the magnitude of these shear and hence tensile forces developing behind the moving asperities. Therefore, high wear of silicon under dry and grease lubricated test conditions may be correlated with and attributed to the high friction nature of these sliding surfaces. Specifically, because of its very poor fracture toughness, silicon undergoes microfracture and suffers severe wear. Raman spectroscopy of wear tracks formed under dry or grease lubricated test conditions revealed that certain areas were transformed to an amorphous phase. The exact role of such phase transformation in wear is not very clear from the authors results, but depending on the state of stresses or stress distribution over these areas, the

authors findings suggest that some areas within the wear track undergo microfracture, while other areas experience phase transformation. Again, the authors feel that microfracture is the most dominant cause of wear of silicon under dry or grease lubricated sliding conditions.

Under sliding conditions where a base PAO oil was used, the friction coefficient was always less than 0.2. Hence the location of shear forces was shifted from surface to subsurface and the extent of tensile forces developing behind the moving asperities of Si₃N₄ ball was not as high as those existing in dry or grease lubricated contacts. Under such sliding conditions, development of microcracks on sliding surfaces was greatly suppressed and the wear of silicon was mostly dominated by a deformation mechanism. Specifically, under the influence of normal and tangential forces, a phase transformation from Si-I to Si-II phase occurred and since this phase is metallic and highly ductile, it predominantly underwent plastic flow (see Fig. 8(a)). Some features indicative of microfracture were also present but they were mostly associated with crystallographic (or cleavage) planes. Overall, the wear of silicon under oil lubricated sliding conditions was mostly dominated by plastic deformation. In an earlier study, the thickness of the transformed and plastically deformed layers was estimated to be less than one micrometer (Gogotsi, 1999).

CONCLUSIONS

1. Silicon wears mainly by brittle fracture under dry sliding conditions in open air and in dry nitrogen. Under such conditions, limited pressure-induced metallization of silicon can also occur during sliding contact, especially in the very early stages of the run-in period of sliding tests.
2. Microfracture is also a predominant wear mechanism under conditions of grease lubrication. However, plastic flow of the material due to pressure-induced metallization of silicon is also observed in certain areas where brittle fracture had not yet occurred.
3. The major mechanism of silicon wear under conditions of oil lubrication is the formation and subsequent plastic flow of the metallic Si-II phase. Detailed SEM and Raman analyses of sliding surfaces suggested that metallic Si-II phase undergoes viscous and/or viscoplastic flow and may transform into amorphous or crystalline silicon phases behind the moving ball. This phenomenon is particularly inherent to the low-load (i.e., 1 and 2 N) sliding conditions where the cracking initiation threshold is not reached.

ACKNOWLEDGMENTS

This study was performed in the framework of the long-term COBASE (Collaboration in Basic Science and Engineering) grant from the National Research Council. Argonne National Laboratory provided a resident associate appointment for Andriy Kovalchenko. Yury Gogotsi was supported by the National Science Foundation Grant DMI No. 0196369.

The SEM analysis was performed in the Electron Microscopy Center, Materials Science Division, Argonne National Laboratory, Argonne, Illinois.

REFERENCES

- (1) Bhushan, B. and Li, X. (1997), "Micromechanical and Tribological Characterization of Doped Single-Crystal Silicon and Polysilicon Films for Microelectromechanical Systems Devices," *Jour. Mater. Res.*, **12**, 1, pp 54-63.
- (2) Blackley, W. S. and Scattergood, R. O. (1994), "Chip Topography for Ductile-Regime Machining of Germanium," *Jour. Eng. Ind.*, **116**, pp 263-266.
- (3) Blake, P. N. and Scattergood, R. O. (1990), "Ductile-Regime Machining of Germanium and Silicon," *Jour. Am. Ceram. Soc.*, **73**, pp 949-957.
- (4) Bradby, J. E., Williams, J. S., Wong-Leung, J., Swain, M. V. and Munroe, P. (2001), "Mechanical Deformation in Silicon by Micro-Indentation," *Jour. Mater. Res.*, **16**, 5, pp 1500-1507.
- (5) Callahan, D. L. and Morris, J. C. (1992), "The Extent of Phase Transformation in Silicon Hardness Indentations," *Jour. Mater. Res.*, **7**, 7, pp 1614-1617.
- (6) Clarke, D. R., Kroll, M. C., Kirchner, P. D., Cook, R. F. and Hockey, B. J. (1988), "Amorphization and Resistance of Silicon and Germanium Induced by Indentation," *Phys. Rev. Lett.*, **60**, 21, pp 2156-2159.
- (7) Danyluk, S., Lee, S. W., Ahn, J. H. and Kahn, A. (1988), "Resistivity of Linear Scratches in Doped (100) *n*-Type Single-Crystal Silicon," *Jour. Appl. Phys.*, **63**, pp 4569-4571.
- (8) Domnich, V. and Gogotsi, Y. (2001a), "Chapter 5: High-Pressure Surface Science," *Handbook of Surfaces and Interfaces of Materials*, Academic Press, Nalwa, H. S., ed., pp 195-237.
- (9) Domnich, V. and Gogotsi, Y. (2001b), "Pressure-Induced Phase Transformations in Semiconductors under Contact Loading," *Frontiers of High-Pressure Research II: Application of High Pressure to Low Dimensional Novel Electronic Materials*, Kluwer Academic Publishers, Dordrecht, N. L., Hochheimer, H. D., Kuchta, B., Dorhout, P. K. and Yarger, J. L., eds., pp 291-302.
- (10) Domnich, V., Gogotsi, Y. and Dub, S. (2000), "Effect of Phase Transformations on the Shape of the Unloading Curve in the Nanoindentation of Silicon," *Appl. Phys. Lett.*, **76**, 16, pp 2214-2216.
- (11) George, A. (1999), "High Pressure Phases of c-Si," *Properties of Crystalline Silicon*, INSPEC, the Institution of Electrical Engineers, London, Hull, R., ed., pp 104-107.
- (12) Gogotsi, Y., Baek, C. and Kirscht, F. (1999), "Raman Microspectroscopy Study of Processing-Induced Phase Transformations and Residual Stress in Silicon," *Semicond. Sci. Tech.*, **14**, 10, pp 936-944.
- (13) Gogotsi, Y., Zhou, G., Ku, S. S. and Cetinkunt, S. (2001), "Raman Microspectroscopy Analysis of Pressure-Induced Metallization in Scratching of Silicon," *Semicond. Sci. Tech.*, **16**, 5, pp 345-352.
- (14) Gogotsi, Y. G., Domnich, V., Dub, S. N., Kailer, A. and Nickel, K. G. (2000), "Cyclic Nanoindentation and Raman Microspectroscopy Study of Phase Transformations in Semiconductors," *Jour. Mater. Res.*, **15**, 3, pp 871-879.
- (15) Gogotsi, Y. G., Kailer, A. and Nickel, K. G. (1997), "Phase Transformations in Materials Studied by Micro-Raman Spectroscopy of Indentations," *Mater. Res. Innov.*, **1**, 1, pp 3-9.
- (16) Gridneva, I. V., Milman, Y. V. and Trefilov, V. I. (1972), "Phase Transition in Diamond-Structure Crystals During Hardness Measurements," *Phys. Stat. Sol. (a)*, **9**, 14, pp 177-182.
- (17) Gupta, M. C. and Ruoff, A. L. (1980), "Static Compression of Silicon in the [100] and In The [111] Directions," *Jour. Appl. Phys.*, **51**, 2, pp 1072-1075.
- (18) Hamilton, G. M. and Goodman, L. E. (1966), "The Stress Field Created by a Circular Sliding Contact," *Jour. Appl. Mech.*, **33**, pp 371-376.
- (19) Hanfland, M. and Syassen, K. (1990), "Raman Modes of Metastable Phases of Si and Ge," *High Pressure Res.*, **3**, pp 242-244.
- (20) Kailer, A., Gogotsi, Y. G. and Nickel, K. G. (1997), "Phase Transformations of Silicon Caused by Contact Loading," *Jour. Appl. Phys.*, **81**, 7, pp 3057-3063.
- (21) Kim, S. H. and Danyluk, S. (1990), "4-Point Probe Resistivity Measurements of Dicing Damage in (100) and (111) Single-Crystal Silicon Wafer," *Jour. Mater. Sci.*, **25**, 11, pp 4892-4897.
- (22) Li, Y. and Danyluk, S. (1996), "Dynamic Measurements of Damage Generation in Single Crystal Silicon Due to Sliding Contact with a Spherical Diamond," *Wear*, **200**, pp 238-243.
- (23) Maley, N., Beeman, D. and Lannin, J. S. (1988), "Dynamics of Tetrahedral Networks: Amorphous Si and Ge," *Phys. Rev. B*, **38**, 15, pp 10611-10622.
- (24) Minowa, K. and Sumino, K. (1992), "Stress-Induced Amorphization of a Silicon Crystal by Mechanical Scratching," *Phys. Rev. Lett.*, **69**, 2, pp 320-322.
- (25) Mishina, H. (1988), "Friction and Wear of Semiconductors in Sliding Contact with Pure Metals," *Trib. Int.*, **21**, 2, pp 76-82.
- (26) Morris, J. C. and Callahan, D. L. (1994), "Origins of Microplasticity in Low-Load Scratching of Silicon," *Jour. Mater. Res.*, **9**, pp 2907-2913.
- (27) Olijnyk, H. and Jephcoat, A. P. (1999), "Effect of Pressure on Raman Spectra of Metastable Phases of Si and Ge," *Phys. Stat. Sol. (b)*, **211**, pp 413-420.

- (28) Park, D. -S., Danyluk, S. and McNallan, M. J. (1991), "Friction and Wear of Single-Crystal Silicon at Elevated Temperatures," *Jour. Mater. Sci.*, **26**, pp 1505-1511.
- (29) Pharr, G. M., Oliver, W. C., Cook, R. F., Kirchner, P. D., Kroll, M. C., Dinger, T. R. and Clarke, D. R. (1992), "Electrical Resistance of Metallic Contacts on Silicon and Germanium During Indentation," *Jour. Mater. Res.*, **7**, pp 961-972.
- (30) Roberts, S. G. (1999), "Fracture and Brittle-Ductile Transition in Si," *Properties of Crystalline Silicon*, INSPEC, the Institution of Electrical Engineers, London, Hull, R., ed., pp 144-148.
- (31) Scott, C. G. and Danyluk, S. (1992), "Examination of Silicon Wear Debris Generated in a Linear Scratch Test," *Wear*, **152**, pp 183-185.
- (32) Tanikella, B. N., Somasekhar, A. H., Sowers, A. T., Nemanich, R. J. and Scattergood, R. O. (1996), "Phase Transformations During Microcutting Tests on Silicon," *Appl. Phys. Lett.*, **69**, 19, pp 2870-2872.
- (33) Weppelmann, E. R., Field, J. S. and Swain, M. V. (1993), "Observation, Analysis and Simulation of the Hysteresis of Silicon Using Ultra-Micro-Indentation with Spherical Indenters," *Jour. Mater. Res.*, **8**, pp 830-840.
- (34) Zanolina, E. and Danyluk, S. (1993), "Ball-On-Flat Reciprocating Sliding Wear of Single-Crystal, Semiconductor Silicon at Room Temperature," *Wear*, **162-164**, pp 332-338.
- (35) Zanolina, E., Danyluk, S. and McNallan, M. (1995a), "Effects of Length, Diameter and Population Density of Tribological Rolls on Friction between Self-Mated Silicon," *Wear*, **181-183**, pp 784-789.
- (36) Zanolina, E. S., Danyluk, S. and McNallan, M. J. (1995b), "Formation of Cylindrical Sliding-Wear Debris on Silicon in Humid Conditions and Elevated Temperatures," *Trib. Trans.*, **38**, 3, pp 721-727.